Received: 23 December 2021 | Accepted: 3 November 2022

DOI: 10.1002/2688-8319.12197

Ecological Solutions and Evidence | BRITISH ECOLOGICAL SOCIETY

RESEARCH ARTICLE

Laser scanning reveals potential underestimation of biomass carbon in temperate forest

Kim Calders[1] | Hans Verbeeck[1] | Andrew Burt[2,3] | Niall Origo[4] | Joanne Nightingale[4] | Yadvinder Malhi[5] | Phil Wilkes[2,6] | Pasi Raumonen[7] | Robert G. H. Bunce[8,†] | Mathias Disney[2,6]

[1]CAVElab - Computational & Applied Vegetation Ecology, Department of Environment, Ghent University, Gent, Belgium

[2]UCL Department of Geography, London, UK

[3]Sylvera Ltd., London, UK

[4]National Physical Laboratory, Climate and Earth Observation Group, Teddington, Middlesex, UK

[5]Environmental Change Institute, School of Geography and the Environment, University of Oxford, Oxford, UK

[6]NERC National Centre for Earth Observation (NCEO), UK

[7]Mathematics, Faculty of Information Technology and Communication Sciences, Tampere University, Tampere, Finland

[8]Estonian University of Life Science, Tartu, Estonia

Correspondence
Kim Calders, CAVElab - Computational & Applied Vegetation Ecology, Department of Environment, Ghent University, B-9000 Gent, Belgium.
Email: kim.calders@ugent.be

Handling Editor: Javier Cabello

Funding information
European Metrology Programme for Innovation and Research (EMPIR), Grant/Award Number: 19ENV07 MetEOC-4; H2020 European Research Council, Grant/Award Number: 321131; NERC National Centre for Earth Observation; European Metrology Research Programme, Grant/Award Number: ENV55; Marie Sklodowska-Curie Actions, Grant/Award Number: 835398; Jackson Foundation; Finland Centre of Excellence in Inverse Modelling and Imaging; Belgian Federal Science Policy Office, Grant/Award Number: SR/02/355

Abstract

1. Quantifying climate mitigation benefits of biosphere protection or restoration requires accurate assessment of forest above-ground biomass (AGB). This is usually estimated using tree size-to-mass allometric models calibrated with harvested biomass data.
2. Using three-dimensional laser measurements across the full range of tree size and shape in a typical UK temperate forest, we show that its AGB is 409.9 t ha^{-1}, 1.77 times more than current allometric model estimates. This discrepancy arises partly from the bias towards small trees in allometric model calibration: 50% of AGB in this forest was in less than 7% of the largest trees (stem diameter > 53.1 cm), all larger than the trees used to calibrate the widely used allometric model.
3. We present new empirical evidence that the fundamental assumption of tree size-to-mass scale-invariance is not well-justified for this kind of forest. This leads to substantial biases in current biomass estimates of broadleaf forests, not just in the UK, but elsewhere where the same or similar allometric models are applied, due to overdependence on non-representative calibration data, and the departure of observed tree size-to-mass from simple size-invariant relationships.
4. We suggest that testing the underlying assumptions of allometric models more generally is an urgent priority as this has wider implications for climate mitigation

[†]Died in April 2022.

This is an open access article under the terms of the Creative Commons Attribution License, which permits use, distribution and reproduction in any medium, provided the original work is properly cited.
© 2022 The Authors. *Ecological Solutions and Evidence* published by John Wiley & Sons Ltd on behalf of British Ecological Society.

through carbon sequestration. Forests currently act as a carbon sink in the UK. However, the anticipated increase in forest disturbances makes the trajectory and magnitude of this terrestrial carbon sink uncertain. We make recommendations for prioritizing measurements with better characterized uncertainty to address this issue.

KEYWORDS
three-dimensional modelling, allometry, biomass, carbon, climate, forests, laser scanning

1 | INTRODUCTION

Temperate forests can be substantial reservoirs of carbon (Ciais et al., 2008). They account for approximately 14% of global forest carbon (C) stocks in their biomass and soil, 118.6 ± 6.3 Pg C (Pan et al., 2011). However, accurate estimates of forest carbon stocks and changes in these stocks might be impeded by the current methods that are used for these estimates (Contestabile, 2012).

Typically, estimates of biomass carbon stocks are derived from tree biomass, simply multiplied by 0.5 – the carbon fraction of the tree biomass (Matthews, 1993). Biomass is rarely directly measured at a large scale: instead, allometric size-to-mass models are used to calculate above-ground biomass (AGB) from more easily measurable properties of stem diameter, *D*, and sometimes tree height, *H*. The allometric models are calibrated from destructive measurements of AGB (harvesting and weighing) along with *D* and *H*. However, direct harvest measurements are difficult and expensive, potentially impossible in long-term plots and national parks and are therefore not regularly done, if at all. As a result, there is a heavy dependence on sparse datasets for generalization of large-scale AGB estimates (Vorster et al., 2020). Remote sensing-based estimates of forest biomass rely on these plot-based calculations of biomass for calibration and validation (Avitabile et al., 2016); hence any biases in plot-based estimates propagate into biases in global forest biomass estimation. Moreover, plot- or remote sensing-based estimates of forests are used to estimate biomass carbon emissions or sinks from land use change, the net effect of which is estimated to account for 14% of anthropogenic carbon emissions (Friedlingstein et al., 2020).

Calibration datasets for the development of allometric models are often biased towards smaller trees, which are easier to harvest, cut and weigh and extrapolation through regression is employed for bigger trees (Zianis et al., 2005). If the fundamental assumption of allometry holds, that is that the widely assumed correlation between tree size and mass is independent of tree size, then a bias towards smaller trees in calibration should not matter (Smith, 1980). However, the combination of allometric models that appear effective, particularly on smaller trees, and the arduous nature of harvest measurement, means that this assumption is rarely if ever tested on large trees (Zhou et al., 2021). Therefore, there is potentially a significant problem because models are being applied very widely, beyond (often well beyond) the size and geographical range of their calibration data.

Taking the island of Great Britain as an example of the links between allometric models and national biomass carbon estimates, the total carbon in temperate forests (above-ground and below-ground living material of trees ≥7 cm *D*) in Great Britain is estimated to be 213 Mt C, of which 48.8% is stored in broadleaved trees (Forestry Commission, 2014a), with approximately 71.5 Mt C carbon in above-ground tree parts. However, these carbon stock estimates for many broadleaved tree species depend almost exclusively on a single calibration dataset generated in the 1960s by Bunce (1968), containing just over 200 destructively sampled trees across five different species (*Acer pseudoplatanus*, *Fraxinus excelsior*, *Quercus* spp., *Tilia cordata* and *Betula* spp.) felled at four localities (Meathop Wood, Roudsea Wood, Coniston, Force Forge) in the English Lake District. Even though sampling by Bunce was done across the full tree size range at those localities at the time, the dataset does not cover anywhere near the size range in other locations (Figure 1) nor does it reflect the present state of trees that have experienced over half a century of growth under changing climatic influences (Kirby et al., 2014). The models developed by Bunce using these regionally specific (and size-limited) calibration data, have been widely used across Great Britain and beyond (Supplementary Table S1), an approach that is widespread for reasons we discuss below. This includes at least 20 other studies, seven of which are outside the UK, none of which are in similar forests. Furthermore, a synthesis of 607 allometric biomass models used across Europe (Zianis et al., 2005) lists the Bunce allometric models as the only one available to derive above-ground woody biomass for the widespread and abundant tree species *A. pseudoplatanus*, *Fraxinus excelsior* and *T. cordata*.

Here we used terrestrial laser scanning (TLS, also terrestrial LiDAR) methods and three-dimensional (3D) analysis to derive tree volume (*V*) non-destructively and further convert this to AGB and carbon (Calders, Newnham et al., 2015) in order to assess the reliability of allometry-based estimates of biomass in a temperate forest. We then further test underlying assumptions in allometric models more generally to investigate and understand potential discrepancies in biomass estimates and the wider implications of this study using UK temperate forest AGB as an example. These outcomes are extremely important for ongoing and forthcoming space missions aimed at reducing uncertainty in global forest biomass and carbon that currently depend on allometric models for calibration and validation (Duncanson et al., 2021). At more local and regional scales, better and more certain baseline measurements of carbon stocks are essential to quantify the impact of an anticipated

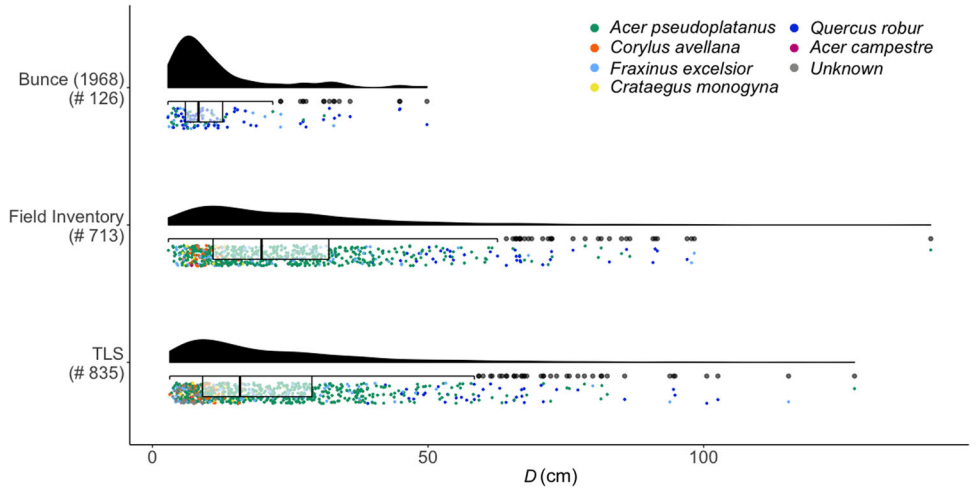

FIGURE 1 Bias towards smaller trees in the calibration data of allometric models in UK temperate forests. Full diameter (*D*) distributions of our study area of Wytham Woods (UK) according to the field inventory and TLS (terrestrial laser scanning) data in 2015 compared to the *D* distribution of destructively sampled trees in the English Lake District that are used to construct allometric AGB models in Bunce (1968). Values from Bunce (1968) were systematically digitized using WebPlotDigitizer (https://automeris.io/WebPlotDigitizer/) for *A. pseudoplatanus*, *F. excelsior* and *Quercus* spp. Boxplot whiskers indicate 1.5 times the interquartile box plot range. Non-uniform allometric model calibration data are typical. For example, a widely used pan-tropical allometric model (Chave et al., 2014) demonstrates an AGB range from 1 to 76,064 kg with the median and mean values being 98 and 1134 kg (A. Burt et al., 2020).

increase in forest disturbances on the trajectory and magnitude of carbon stocks.

2 | MATERIALS AND METHODS

2.1 | Study area and data collection

The 1.4-ha study area was located within Wytham Woods, Oxford, UK, and is part of a larger 18-ha Smithsonian plot that is run by Oxford University (https://www.forestgeo.si.edu/sites/europe/wytham-woods, Supplementary Figure S1). The forest is dominated by *Fraxinus excelsior*, *A. pseudoplatanus* and *Corylus avellana*. The mean annual rainfall is 726 mm, the mean annual temperature is 10°C and the mean annual radiation is 118 W m^{-2} (Butt et al., 2009). Wytham Woods is a typical temperate forest site in southern Great Britain (Kirby et al., 2014; Savill et al., 2011), and its *D* distribution (Figure 1) is representative for broadleaved woodlands in Great Britain (Forestry Commission, 2013).

TLS is an active remote sensing technique that captures the environment in three dimensions by emitting millions of laser pulses (Calders et al., 2020). A 3D point cloud is generated through analysis of the elapsed time between emission and detection of laser pulses that are reflected back to the TLS instrument. TLS data were collected in leaf-off conditions throughout late November 2015, December 2015 and January 2016. Windy days were avoided to ensure data quality. We used a RIEGL VZ-400 terrestrial laser scanner (RIEGL Laser Measurement Systems GmbH). The instrument has a beam divergence of 0.35 mrad and operates in the infrared (wavelength 1550 nm) with a range up to 350 m. The pulse repetition rate for each scan was 300 kHz, the minimum range was 0.5 m and the angular sampling resolution was 0.04°. This resulted in 22,500,000 outgoing pulses for a single scan, resulting in a beam diameter of 2.45 cm and beam spacing of 3.5 cm at 50 m (for instance). The azimuth angle range was 0°–360°, and the zenith angle range was 30°–130°. Therefore, an additional scan was acquired at each scan location with the scanner tilted at 90° from the vertical to complete sampling of the full hemisphere at each location. Scans were done in a larger 6 ha area using an approximate 20 m × 20 m grid to ensure the best possible data quality within our 1.4 ha study area (Wilkes et al., 2017). Trees which had at least more than half of their stem at tree diameter 1.3 m inside the boundaries of the study area were included.

2.2 | TLS-derived structural metrics and carbon stocks

Analysis of single trees from a co-registered point cloud required tree segmentation. When a multi-stem tree splits into single stems below 1.3 m, each stem was considered to be an individual tree in the analysis. Tree segmentation used the open-source software *treeseg* (A. Burt et al., 2018), followed by visual inspection to ensure that every tree is segmented correctly. *Treeseg* is mainly data-driven and uses few a priori assumptions about tree architecture. This approach uses generic point cloud processing techniques, such as principal component analysis, region-based segmentation, Euclidean clustering, shape fitting and connectivity testing. Full details of each step involved in the tree segmentation can be found in Calders et al. (2018).

2.2.1 | Structural metrics

Tree height, *H*, was calculated as the difference between the height of the highest and lowest LiDAR point of a single tree point cloud. The diameter at breast height, *D*, was calculated on a 0.06-m thick cross section between 1.27 and 1.33 m above the lowest point through a least squares circle fitting algorithm to account for potential occlusion in the LiDAR data (Calders, Newnham et al., 2015). A quality check was performed on this initial estimate of *D*. These quality criteria thresholds removed obviously incorrect fits for those distorted by a few outlier points, occluded regions or cross sections that were too far removed from a perfect circular shape (Supplementary S2.2). A total of 661 trees passed these *D* quality criteria, and for the 174 other trees *D* was derived from the quantitative structure models (QSMs) stem cylinder at 1.3 m. Alpha shapes (concave hull) were calculated using the *shapely* package in *python v3.7.6* (Python Software Foundation, n.d.). Crown area (*CA*) is derived from the vertical projection of the full point cloud using alpha shapes.

2.2.2 | Carbon stocks

3D measurements of trees through TLS methods were combined with geometric modelling to estimate their volume (Calders, Newnham et al., 2015). Isolating individual trees from a forest point cloud followed by enclosing points with geometric shapes results in a volume estimate of the tree, which can be converted to mass using the wood density. We collected leaf-off TLS data (i.e. in the winter in a deciduous forest) to ensure capture of all woody components of the trees (stem, branches) and minimize the impact of leaves on the point cloud (Boni Vicari et al., 2019; Krishna Moorthy et al., 2020).

Individual leaf-off tree point clouds are enclosed with geometric shapes to create QSMs that allow volume calculations. Here, we used the *TreeQSM v2.0* workflow (https://github.com/InverseTampere/TreeQSM) described in Calders, Newnham et al. (2015). This approach builds on Raumonen et al. (2013) and fits cylinders to the branch segmented point cloud data (Supplementary Figure S2). The most important input parameter in QSM reconstruction is the cover patch size, which defines the size of the building blocks to model the tree branches from the base up. We optimized the patch size automatically using a modified version of Calders, Burt et al. (2015) and we refer to Calders et al. (2018) for a step-by-step description of this approach. Once the optimal patch size has been determined, the modelling procedure produces multiple QSM iterations for each tree with this patch size to quantify the QSM model fitting uncertainty (as a stochastic fitting process). From these multiple iterations of whole-tree volume estimations (*V*), a standard deviation, which is representative of the QSM model fitting uncertainty, is produced. In order to propagate this uncertainty from tree level *i* (V_i) through to the plot estimates ($V_{alltrees}$), we utilized the law of propagation of uncertainties (JCGM, 2008) without the correlation terms:

$$u^2\left(V_{alltrees}\right) = \sum_{i=1}^{N}\left(\frac{\partial V_{alltrees}}{\partial V_i}\right)^2 u^2\left(V_i\right), \quad (1)$$

where $u(V_{alltrees})$ is the uncertainty of the final estimate ($V_{alltrees}$) for the total number of trees (*N*), $\frac{\partial V_{alltrees}}{\partial V_i}$ gives the sensitivity coefficients, and $u(V_i)$ gives the uncertainty associated with the inputs (V_i).

To scale this to per hectare (V_{ha}) estimates, we use

$$u^2\left(V_{ha}\right) = \left(\frac{\partial V_{ha}}{\partial V_{alltrees}}\right)^2 u^2\left(V\right), \quad (2)$$

$$\text{where } \left(\frac{\partial V_{ha}}{\partial V_{alltrees}}\right) = \frac{1}{1.4}.$$

Model uncertainties were given with a coverage factor of 2, which is equal to approximately 95% confidence level according to a Gaussian distribution.

A conversion of QSM volume to mass was done using species-specific wood density values. Tree species were identified by matching TLS tree maps with field inventory coordinates of trees. Wood density values were taken from McKay et al. (2003) for the three dominant species *A. pseudoplatanus*, *F. excelsior* and *Q. robur*, and from the DRYAD database (Zanne et al., 2009) for the other three species (*Corylus avellana*, *Crataegus monogyna*, *A. campestre*). Seventy-one trees could not be assigned a species as they were generally too small to be included in the field inventory, and a weighted wood density was used for these trees (Supplementary Table S2). Conversion of volume into AGB through wood density adds uncertainties to AGB estimates, caused by high inter-, intra-species and within-tree variability of wood density (Demol et al., 2021). The carbon density of (dry) biomass is often approximated at 50% for trees found in British and European forests (Matthews, 1993; Nabuurs et al., 2007). Here, we use species-specific values of carbon density derived in Wytham Woods (Butt et al., 2009; Fenn et al., 2015). The overall mean carbon densities were 49.07% for *Fraxinus excelsior*, 47.40% for *Q. robur*, 46.89% for *A. pseudoplatanus* and 47.79% for the remaining species.

TreeQSM has been benchmarked against other QSM methods (Hackenberg et al., 2015), as well as destructive measurements of smaller (A. P. Burt, 2017; Calders, Newnham et al., 2015) and larger trees (A. Burt et al., 2021; de Tanago Menaca et al., 2018; Momo Takoudjou et al., 2018). However, most of these studies used leaf-on TLS data, reporting slight overestimations of TLS-derived AGB compared to destructive measurements. Calders, Newnham et al. (2015) reported a total AGB overestimation of 9.7% to the reference measurement compared to an underestimation of 29.9–36.6% for allometric models in native Eucalypt Open Forest (dry sclerophyll Box-Ironbark forest) in Victoria, Australia. Momo Takoudjou et al. (2018) reported a bias of 4.7% when comparing optimized QSM with destructive measurements in Cameroon. Gonzalez de Tanago et al. (2018) reported a small underestimation (bias −3.7%) when comparing QSMs against

destructive harvesting for a range of tropical trees across Peru, Guyana and Indonesia. A. Burt et al. (2021) demonstrated the importance of using leaf-off (or removal of leaves in leaf-on) TLS data for estimating woody AGB (using the same RIEGL VZ-400 instrument used in this study). Using destructive harvesting of trees in Brazil, A. Burt et al. (2021) reported mean relative errors indicating a TLS AGB overestimation of 42% for leaf-on QSMs and a 3% underestimation for the leaf-off QSMs.

2.3 | Allometric tree volume model evaluation using TLS data

Here we fitted new allometric models using the TLS estimates of tree volume as calibration data: species-specific for *A. pseudoplatanus* and a generic (non-species-specific) model. Structural characteristics of these trees are described in Supplementary Table S3. We calculated a species-specific model for *A. pseudoplatanus* due to its large sample size.

We used ordinary least squares (OLS; *lm* package in R version 3.6.3) to fit the following models with the data:

$$\text{Model 1 } (m1): \ln(V) = a_0 + a_1 \ln(D) + \varepsilon,$$

$$\text{Model 2 } (m2): \ln(V) = b_0 + b_1 \ln(D) + b_2 \ln(H) + \varepsilon,$$

$$\text{Model 3 } (m3): \ln(V) = c_0 + c_1 \ln(D) + c_2 \ln(H) + c_3 \ln(CA) + \varepsilon.$$

Units are V (m^3), D (m), H (m) and CA (m^2). ln is the natural logarithm, and ε describes the random error of the model. Model *m1* is used to establish the Bunce allometric models. Similar to A. Burt et al. (2020), multivariate models *m2* and *m3* add more complexity, given the structural parameters that are derived from TLS. *D*, *H* and *CA* are independent observations of individual trees and derived from the TLS data. OLS was selected over more robust methods despite 'outliers' (see Supplementary Figures S4 and S5), because these are perfectly reasonable observations of individual trees, and there is no justification for their exclusion, which would otherwise artificially reduce the variance observed in these forested ecosystems. The lack of large (beyond ± 2) outliers in our data means there should be minimal effect of leverage. However, while in general heteroskedasticity and non-normality do not bias OLS model parameters themselves (Hayashi, 2000; Olvera Astivia and Zumbo, 2019), but can potentially introduce bias in the standard errors. Ideally, tests of heteroskedasticity would be a routine part of fitting allometric models to tree size data. But in the absence of this, care needs to be taken in interpreting out-of-sample predictions and uncertainty (A. Burt et al., 2020). A fundamental assumption of our analysis is that both the expected error in TLS-derived estimates of volume is zero and that individual errors are uncorrelated with one another. If these assumptions do not hold (e.g., the error in the TLS estimates is correlated with tree size), the models are incorrectly specified, and the tests of size invariance are difficult to interpret. We believe this is a reasonable assumption because of evidence accrued from validation studies comparing TLS estimates (derived from the same instrument and processing chain) with direct weighing measurements (Australia – Calders, Newnham et al., 2015; Brazil – A. Burt et al., 2021). Conversion of these models in real-space requires using the widely used Neyman correction factor (Neyman and Scott, 1960), which is based on the OLS estimate of the standard deviation of the error (equation 16 in A. Burt et al., 2020), that is $A_0 = e_0^a e^{\hat{\sigma}^2/2}$, where $\hat{\sigma}$ is the estimated standard deviation.

$$\text{Model 1 } (m1): V = A_0 D^{a_1}$$

$$\text{Model 2 } (m2): V = B_0 D^{b_1} H^{b_2}$$

$$\text{Model 3 } (m3): V = C_0 D^{c_1} H^{c_2} CA^{c_3}.$$

Confidence intervals for these parameters were constructed using a BCa bootstrap (95%, 10,000 iterations replicates in R using *set.seed(123)*, Supplementary Table S4). Note that *D*, *H* and *CA* are derived from TLS measurements and that the use of other measurement techniques will introduce inconsistent measurement error (as per A. Burt et al., 2020).

A repeated (10 times) stratified 10-fold cross-validation was used to assess model uncertainties: the median symmetric accuracy (i.e. percentage error) and the symmetric signed percentage bias (percentage bias) were conducted (Supplementary Table S5).

3 | RESULTS

3.1 | TLS-derived carbon stocks

The total QSM-derived volume for all 815 live standing trees (Figure 2) is 1039.6 ± 5.4 m^3, which equates to 742.6 ± 3.9 m^3 ha^{-1}. The relatively low (<1%) model uncertainties are due to the high point cloud quality, which can be mostly attributed to the leaf-off data acquisition conditions. Leaf-on TLS data will increase occlusion in the data and requires an additional processing step to remove leaves using leaf-wood separation algorithms (Béland et al., 2014; Boni Vicari et al., 2019; Krishna Moorthy et al., 2020; Wang et al., 2020), which will introduce additional uncertainty.

TLS-derived AGB was 573.8 tonnes in total for all live standing trees, which equates to 409.9 t ha^{-1} (Figure 3). This is significantly more than the 231.9 t ha^{-1} resulting from the Bunce allometric models that are commonly used in these temperate forests (Bunce, 1968; Butt et al., 2009; Forestry Commission, 2014a, 2014b) and that have been applied previously at this same site for biomass estimation (Supplementary Table 1). The agreement between individual tree AGB estimated through TLS data and allometric models shows a concordance correlation coefficient (CCC) of 0.77 (Figure 3). Overall, TLS-derived AGB is larger than estimates from allometric models, even for trees that fall within the size range of the allometric calibration data. However, AGB residuals increase for trees with larger diameters (Supplementary Figure S3). This is similar to previous findings (Calders, Newnham et al., 2015; de Tanago Menaca

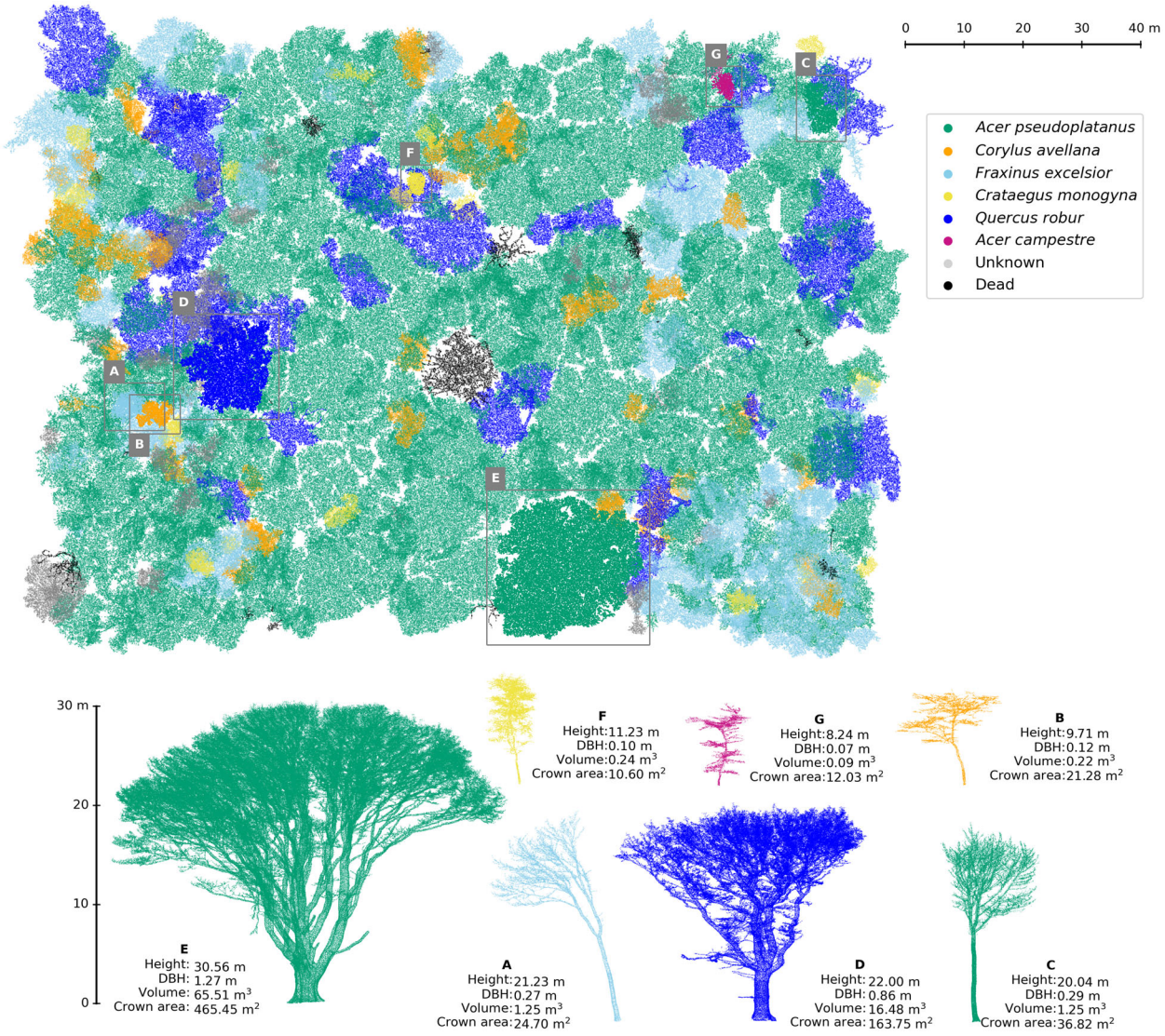

FIGURE 2 3D TLS data. (top) top-of-canopy view of 835 trees in the 1.4 ha study area coloured by species. (bottom) side view of individual trees. A 3D view of these trees and their QSMs can be found in Supplementary Figure S2.

et al., 2018), but the magnitude of the residuals is much larger for our dataset.

Further conversion of our TLS-derived AGB values using species-specific carbon densities results in an estimate of 194 t ha^{-1} of carbon. This translates to 1.77 times more carbon when compared to carbon values derived through the allometric AGB models developed by Bunce.

3.2 | Allometric tree volume model evaluation using TLS data

As sessile organisms, trees have a significant ability to adjust their phenotype in response to different environmental conditions, that is their so-called plasticity (Laitinen and Nikoloski, 2019; Loubota Panzou et al., 2020). Even within our study area, trees of the same species express extraordinary plasticity (Figure 4). Here, we explored the impact of this plasticity on three different allometric model forms. We optimized each model form for *A. pseudoplatanus* (n = 532) as well as a generic model (all living trees, n = 815) that can be applied across species. Model *m3* performed better than the other model forms with a reduction of at least 30% in mean uncertainty and 54% in mean bias (Supplementary Table S5).

4 | DISCUSSION

4.1 | Understanding discrepancies in biomass: Allometric model misuse

AGB allometric models are often constructed using calibration data with certain assumed characteristics (e.g., heavily biased towards small

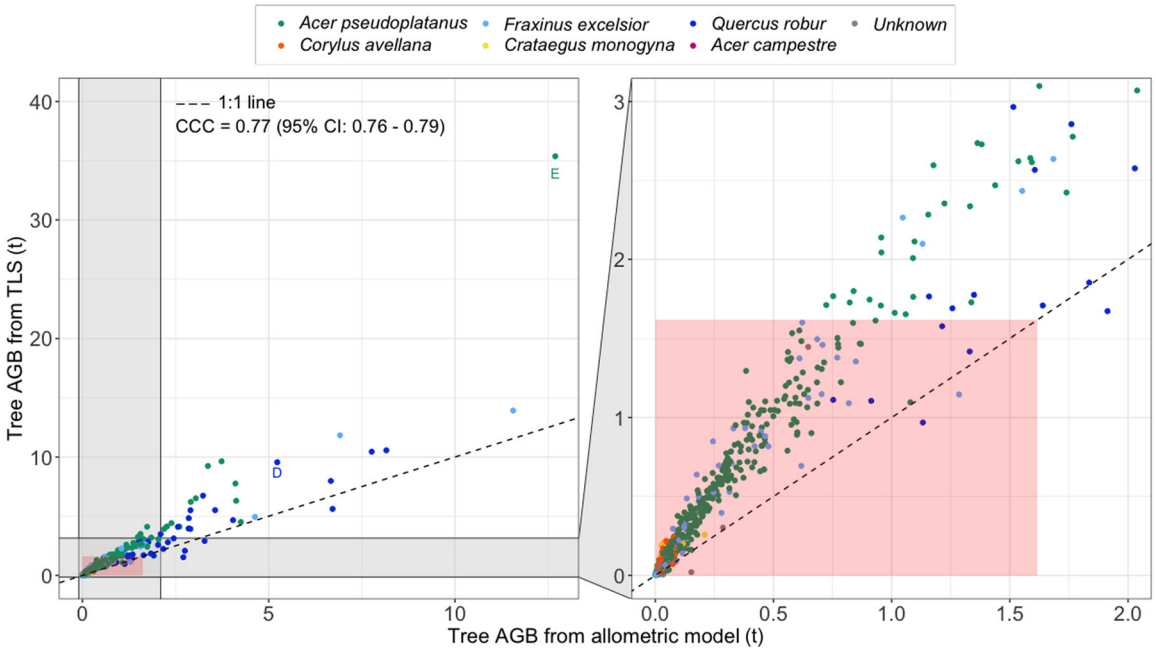

FIGURE 3 Individual tree AGB for Wytham Woods. Direct TLS-derived estimates versus estimates from allometric models using Bunce (1968) and TLS-derived *D*. Bunce allometric model coefficients were similar to previous work in Wytham Woods (Butt et al., 2013; Fenn et al., 2015). Letters D and E relate to the individual trees in Figure 2. CCC is the concordance correlation coefficient (together with its 95% confidence interval) and demonstrates the degree of agreement of two methods and can range between 1 (perfect concordance) and −1 (perfect discordance). The red shaded box indicates the range (1–1617 kg) of destructively measured AGB that underpins the Bunce allometric models.

trees, specific taxa and location), that are inconsistent with trees to which they are applied. We argue that the underlying assumptions used to predict carbon stocks for temperate broadleaved forests in Great Britain, and to some extent across Europe, are likely not met currently due to two key factors: (1) trees do not follow a size-invariant scaling relationship, particularly at larger size; and (2) changes in forest management have increased the abundance of larger trees since the development of these allometric models in the 1960s.

4.1.1 | Size versus volume dependency in allometric models

There is a lack of large trees in the data underpinning the Bunce AGB allometry compared to 2015 field inventory and TLS data that capture all trees within our study area, irrespective of size (Figure 1). The median *D* from Bunce (1968) is 8.4 cm, where this is 15.9 cm for the TLS data and 19.8 cm for the field inventory. The difference between TLS and field inventory is due to the presence of extra (smaller) trees in the TLS data that are not recorded in the field inventory. The median *D* for TLS shifts to 19.2 cm when not accounting for these smaller trees. Larger trees are generally underrepresented due to the impracticality and expense of collecting destructively sampled calibration data, even for allometric models that are applied widely (A. Burt et al., 2020). Most allometric models assume that the relation between size (or some specific, measurable aspect of size such as trunk diameter) and mass is invariant and therefore can be specified using constant model parameters across tree size. However, assessing the validity of this fundamental assumption is difficult because of the aforementioned lack of data from large trees (A. Burt et al., 2020). Systematic error in allometric models has been identified previously in tropical forests (A. Burt et al., 2020; Picard et al., 2015; Ploton et al., 2016) and through global synthesis (Poorter et al., 2015). Inclusion of crown area in allometric models results in lower uncertainties and biases and smaller residuals for larger trees. This supports earlier work on the importance of including crown area in allometric models (Jucker et al., 2017). Our data suggest that, overall, trees with small *D* will first grow in *H*, before expanding their *CA* (Supplementary Figure S6). Recent destructive harvest work combined with TLS has shown that large tropical trees can have 60% of their total mass in their crowns, much more than predicted by allometry calibrated on much smaller trees (A. Burt et al., 2021).

Figure 5 shows the impact of iteratively removing the 10% smallest trees in terms of *V* for model *m1* (i.e. the same model form as used for the Bunce allometric models), followed by refitting the model, and non-parametric calculation of parameter confidence intervals via bootstrapping. When we refit the model, the population also changes by removal of the trees, which can result in slightly different variances between model fits. Confidence intervals for parameters a_0 and a_1 are not in agreement across the whole range (i.e. they do not intersect with every other sample size). There are multiple plausible explanations for this, such as systematic error in the TLS-derived estimates of *V*. However, a growing body of literature is demonstrating that these estimates can be highly accurate. Therefore, a strong candidate for explaining this is that these trees do not follow a size-invariant scaling

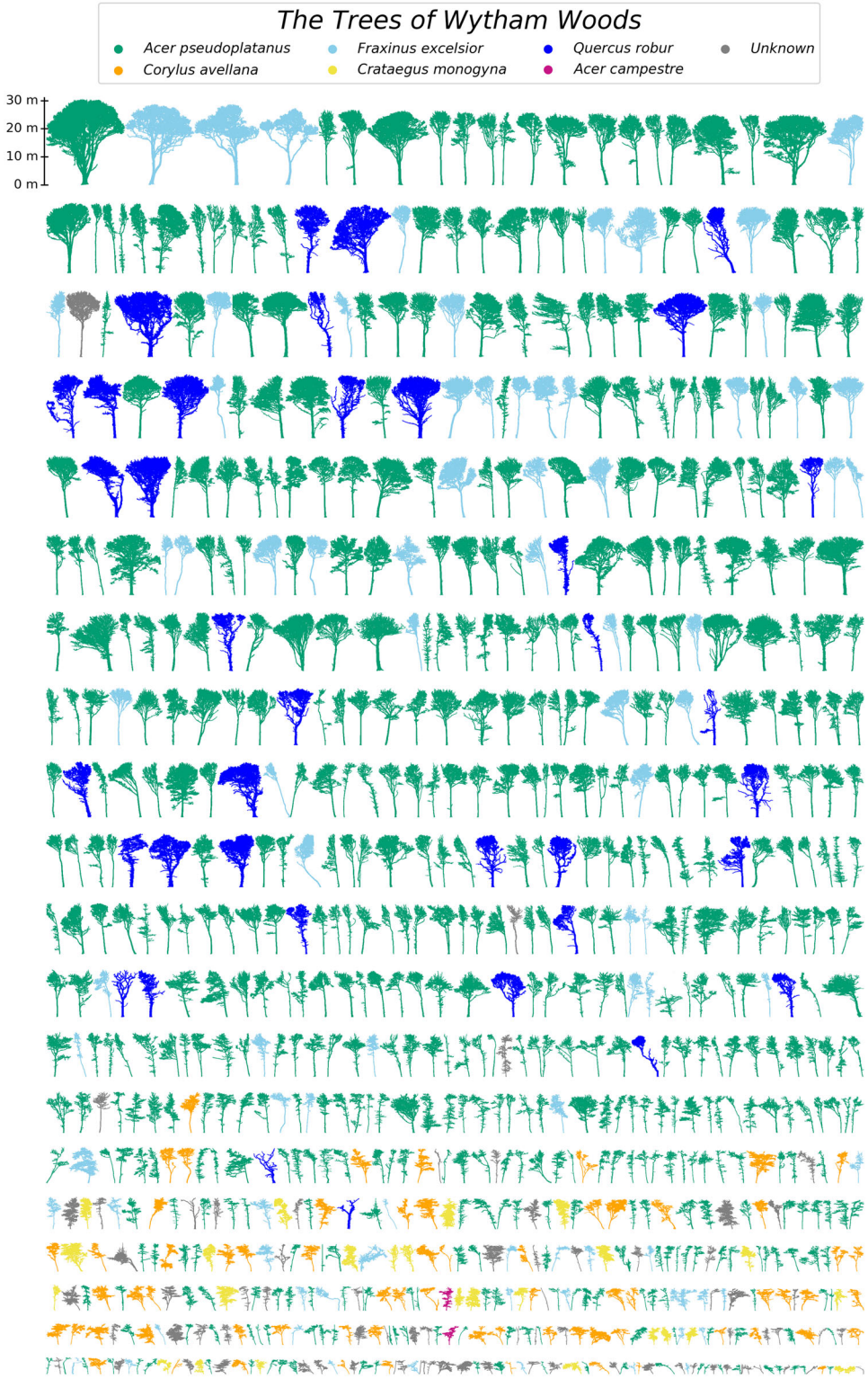

FIGURE 4 Plasticity expressed by the 835 trees of our study area in Wytham Woods. Data (*xz* cross section) from 3D TLS, trees ordered by decreasing height.

relationship between *D* and *V*. Similar results are observed for model *m2* (Supplementary Figure S7) and *m3* (Supplementary Figure S8) with clear trends across size class that are significant for most cases. The implication of this is that predictions from allometric models assuming size-invariance (e.g., Bunce) will induce systematic errors. For this reason, we also want to stress that we did not attempt to provide new, improved allometric models using TLS as calibration data but only to explore the potential mass-size (in)variance of trees. We think this helps explain the substantial discrepancy between the TLS and allometric estimates. Warnings against assuming size dependency are not new

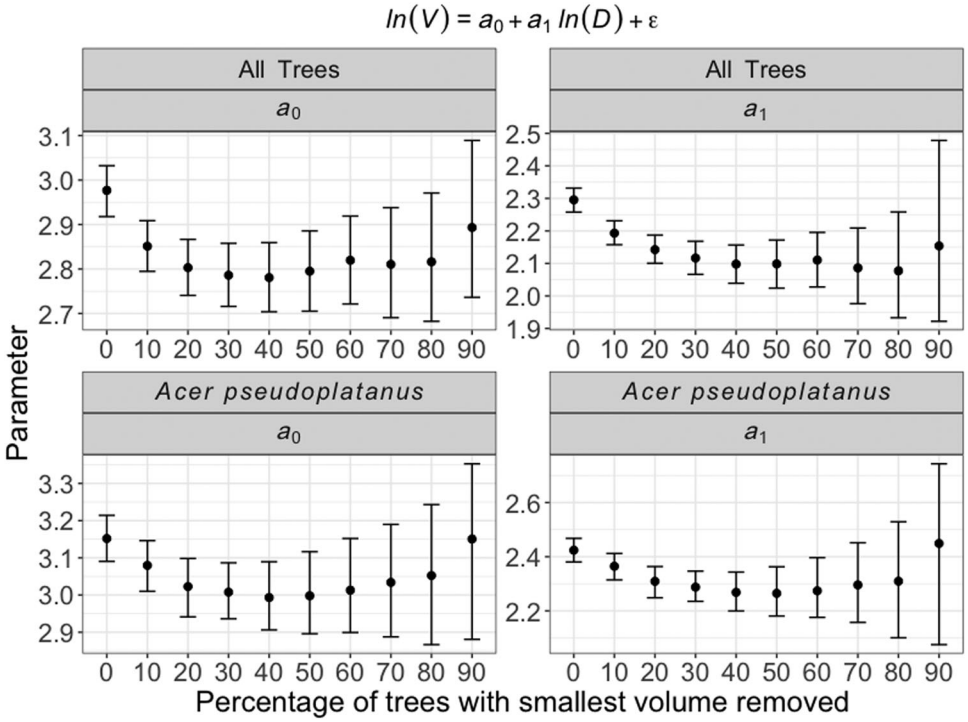

FIGURE 5 Size dependence of allometric model parameters for the trees in Wytham Woods. The 10% smallest trees in terms of volume were iteratively removed and model *m1* was refitted. Bootstrapped 95% confidence intervals ($N = 10{,}000$) are shown for each model parameter. The size of the confidence intervals increases as the sample size decreases, but it can be seen in multiple instances that intervals do not intersect with one another.

(Smith, 1980), but are often ignored. Zhou et al. (2021) present a theoretical framework to characterize allometric models using a dynamic allometric scaling relationship and account for the issue of scaling in different-sized trees; TLS data are likely well-suited to this approach.

4.1.2 | Increased frequency of large trees

Trees compete for light and other resources, and combined with forest management practices and other pressures such as grazing, this determines the overall tree structure in forest stands. The majority of primary (ancient) woodlands were managed under different types of coppice and coppice with standards, with patterns related to local history and conditions with many different structures. Coppice stems were widely used for building material and for making charcoal for iron smelting from the Weald of Kent to the Lake District and to Western Scotland. The majority of these woods have not been managed since the decline of the charcoal industry towards the end of the nineteenth century and are thus usually mixtures of overgrown coppice stools and singled standards. Local felling for timber and firewood, especially in the two World Wars, was a subsequent source of local variation. TLS data collection for this study was in an area of Wytham Woods categorized as '*disturbed ancient woodland*', which was formerly managed as coppice with standards but converted to high forest during the twentieth century (Butt et al., 2009). Very little management has taken place after the 1960s in the area where TLS data were collected in 2015, and the current *D* distribution is representative for broadleaved species in Great Britain (Figure 1 and Forestry Commission, 2013)

Forest structure has undergone significant changes in Great Britain compared to when the Bunce allometric models were established in 1968 based on data collected in actively coppiced woodlands. There has been a general increase in basal area (Kirby et al., 2005) that more than doubled in Wytham Woods in 40 years from 1974 (Kirby et al., 2014). Furthermore, the modal diameter class in Wytham Woods has shifted from 11–20 cm in 1974 to 30–40 cm in 2012 (Kirby et al., 2014), indicating an increased frequency of larger trees in the population, typical of abandoned coppice forest (Rackham, 2015). Analysis of all trees in our study area demonstrates the importance of larger trees in carbon accounting (Figure 6). Less than 2% of the trees account for 25% of the plot-level AGB and less than 7% of trees represent half of the AGB, all larger than those used to calibrate the Bunce allometric model. This complements findings in the tropics that large trees contribute disproportionately to above-ground carbon stocks (Poulsen et al., 2020).

4.2 | Perspective on forest climate mitigation contribution

The trajectory of growth at Wytham Woods strongly reflects the upheavals in management over the past century, most recently during the Second World War (Kirby et al., 2014). This results in a net

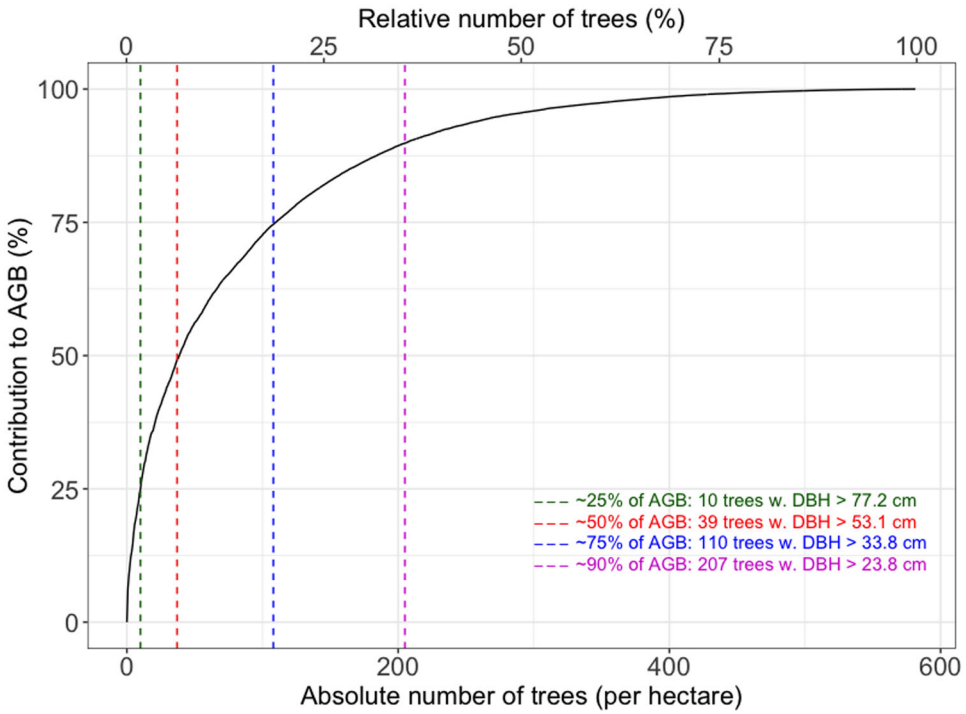

FIGURE 6 Contribution of large trees to plot-level AGB. Numbers of the 1.4 ha study area are scaled to trees per hectare. Individual trees are ranked by decreasing D.

carbon sink of approximately 1 t ha^{-1} $year^{-1}$ ha (unpublished data) using the traditional allometric models from Bunce (1968). Revisiting this estimate based on our 3D analysis results in a net carbon sink of approximately 1.77 t ha^{-1} $year^{-1}$ ha, but this sink may not be sustainable. Ash dieback, caused by the fungal pathogen *Hymenoscyphus fraxineus*, was first observed in the UK in 2012 (Mitchell et al., 2014) and eventually reached Wytham Woods in 2017 (Kirby, 2020). Ash contributed to approximately 13.2% of the biomass carbon in our study area, but its overall presence is close to 34% in a larger 18-ha long-term monitoring plot of which this study area is a part. The impact of ash dieback is expected to be significant since the abundance of ash in regeneration (number of seedlings) increased from 34% in 1974 to 75% in 2012 (Kirby et al., 2014) over the whole of Wytham Woods. Wytham Woods, and in extension a significant amount of European temperate deciduous forests, are likely to have become (or will soon become) a substantial carbon source in the next few years due to ash dieback (Needham et al., 2016).

The global terrestrial carbon sink has increased in the past decades (Ciais et al., 2019). Recent work suggests that the tropical terrestrial carbon sink is declining (Hubau et al., 2020), which highlights the importance of non-tropical forests, particularly in the Northern Hemisphere, for climate mitigation through carbon sequestration. Predicted changes in climate will likely increase forest disturbances (Seidl et al., 2017). These disturbances have a significant impact on the carbon budget; for example, the 2010 Amazon drought event led to 2.2 Pg C committed emissions due to increased tree mortality, as well as subsequent impacts on forest composition and resilience (Lewis et al., 2011). Furthermore, if allometric models underestimate current stocks, as our results here suggest, the magnitude of this carbon source is likely to be substantially larger than anticipated. Reducing uncertainty in forest carbon estimates is vital, given that land use, and forest protection and restoration, in particular, constitutes one quarter of countries' current commitments to their Paris Agreement targets (Grassi et al., 2017). These targets need to take into account the trajectory and magnitude of current carbon stocks in a changing climate (Anderegg et al., 2020). The urgency of this is illustrated by the fact that the UK's biomass stock reporting to the FAO (FAO, 2020; Forestry Commission, 2014b) is still based on Bunce's allometric models for deciduous forest (McKay et al., 2003), almost certainly resulting in significant under-reporting. The three dominant species in our Wytham Woods site contribute to more than 26% of the broadleaved tree AGB and carbon in Great Britain (Forestry Commission, 2014a, 2014b). This problem is almost certainly more widespread; significant allometric underestimates of the biomass of large trees particularly have been reported for *Sequoia sempervirens* (Disney et al., 2020), *Eucalyptus* spp. (Calders, Newnham et al., 2015) and tropical trees in Peru, Indonesia and Guyana (de Tanago Menaca et al., 2018).

5 | OUTLOOK

There are several actions that could be taken to address potential biases in biomass carbon estimates and drastically improve estimates of forest biomass. These actions are

(i) Generate a much greater sample of nondestructive estimates of AGB with TLS, together with a better understanding of wood density

(Demol et al., 2021). These estimates can provide increased sample sizes, with more large trees (A. Burt et al., 2020; Vorster et al., 2020) and, critically, allow for properly testing the fundamental assumption of size dependency in allometric models (A. Burt et al., 2020). Importantly, TLS can be used to capture the full-size distribution of trees within sample plots, rather than having to select a few individuals for destructive harvest.

(ii) Develop empirical models of AGB that do not assume size invariance. This requires potentially moving away from the assumption that a single form will work across all size ranges (Zhou et al., 2021), based on looking at size-biased samples of harvested trees. Models should sample trees across the full-size range and quantify the resulting prediction uncertainty. This implies more destructive harvesting, particularly balanced datasets that cover large size ranges and/or more TLS sampling, but ideally both.

(iii) Establish a biomass reference network of permanent sample plots that are specifically designed for estimating and assessing AGB. This is particularly important given the rapid expansion of satellite-derived biomass estimates, which are likely to become the de facto standard for assessing state and change of forest AGB at large scales. Spaceborne estimates all rely on allometric approaches to some degree, but there is almost nothing in the way of ground-based measurements to calibrate or validate these estimates. GEO-TREES has been proposed as a solution to this (https://earthobservations.org/documents/gwp20_22/GEO-TREES.pdf). The aim is to build on and supplement existing long-term ecological plot networks, but including TLS, airborne laser scanning and other ancillary data (including harvest measurements) to specifically allow for upscaling of AGB and development of new empirical models.

(iv) Ensure much better traceability in the use of allometric models. As we show in this work, due to the challenges of destructive harvest and the apparent but untested size-invariant nature of allometric model fits, allometric models are very often applied at one or even several removes from their original data. Where possible, studies that use published allometric models should clearly identify where the underpinning data were collected and when, the number and size range of trees from which models were derived, and note any assumptions made regarding environmental conditions, wood density etc. This information is needed to allow researchers to reproduce the original model fit and to properly assess how well it ought to work in their particular case. This may mean accepting that models are less likely to be suited for wide general use, but will also highlight where work should be focused to improve models and reduce uncertainty. Database initiatives such as GlobAllomeTree (http://www.globallometree.org/) can help in achieving better traceability.

AUTHOR CONTRIBUTIONS

Conceived and designed the experiments: Kim Calders, and Mathias Disney. Performed the experiments: Kim Calders, Andrew Burt, Niall Origo, Joanne Nightingale, Yadvinder Malhi, Phil Wilkes and Mathias Disney. Analyzed the data: Kim Calders, Andrew Burt, Phil Wilkes, Pasi Raumonen, Mathias Disney. Interpretation of data: Kim Calders, Hans Verbeeck, Andrew Burt, Yadvinder Malhi, Robert G.H. Bunce, Mathias Disney. Wrote the paper: Kim Calders & Mathias Disney led the writing, with input from all authors.

ACKNOWLEDGEMENTS

We thank Keith Kirby for his valuable comments and suggestions on an earlier version of this manuscript. K.C. was funded by the European Union's Horizon 2020 research and innovation programme under the Marie Sklodowska-Curie grant agreement No 835398. H.V. was funded by BELSPO (Belgian Science Policy Office) in the frame of the STEREO III programme - project 3D-FOREST (SR/02/355). P.R. was funded by the Academy of Finland's Centre of Excellence in Inverse Modelling and Imaging. The TLS fieldwork was funded through the Metrology for Earth Observation and Climate project (MetEOC-2), grant number ENV55 within the European Metrology Research Programme (EMRP). The EMRP is jointly funded by the EMRP participating countries within EURAMET and the European Union. Funds for purchase of the UCL RIEGL VZ-400 instrument were provided by the UK NERC National Centre for Earth Observation (NCEO) and UCL Geography. The census of the forest plot was supported by an ERC Advanced Investigator Grant to Y.M. (GEM-TRAIT, grant number 321131). Y.M. is also supported by the Jackson Foundation. N.O. was funded by the MetEOC4 project. This project (19ENV07 MetEOC-4) has received funding from the EMPIR programme co-financed by the Participating States and from the European Union's Horizon 2020 research and innovation programme.

CONFLICT OF INTEREST

The authors declare no known conflicts of interest. Andrew Burt was employed by University College London for the duration of the research and analysis conducted for the preparation of this manuscript and is currently employed by Sylvera Ltd.

DATA AVAILABILITY STATEMENT

The 18 ha Smithsonian plot census data for Wytham Woods can be requested through https://www.forestgeo.si.edu/sites/europe/wytham-woods. TLS data (individual tree point clouds and QSMs) and scripts (analysis and figures) are available at https://doi.org/10.5281/zenodo.7307956.

ORCID

Kim Calders https://orcid.org/0000-0002-4562-2538
Hans Verbeeck https://orcid.org/0000-0003-1490-0168
Andrew Burt https://orcid.org/0000-0002-4209-8101
Niall Origo https://orcid.org/0000-0002-8475-6264
Joanne Nightingale https://orcid.org/0000-0001-7061-4305
Yadvinder Malhi https://orcid.org/0000-0002-3503-4783
Phil Wilkes https://orcid.org/0000-0001-6048-536X
Pasi Raumonen https://orcid.org/0000-0001-5471-0970
Mathias Disney https://orcid.org/0000-0002-2407-4026

REFERENCES

Anderegg, W. R. L., Trugman, A. T., Badgley, G., Anderson, C. M., Bartuska, A., Ciais, P., Cullenward, D., Field, C. B., Freeman, J., Goetz, S. J.,

Hicke, J. A., Huntzinger, D., Jackson, R. B., Nickerson, J., Pacala, S., & Randerson, J. T. (2020). Climate-driven risks to the climate mitigation potential of forests. *Science*, *368*, eaaz7005. https://doi.org/10.1126/science.aaz7005

Avitabile, V., Herold, M., Heuvelink, G. B. M., Lewis, S. L., Phillips, O. L., Asner, G. P., Armston, J., Ashton, P. S., Banin, L., Bayol, N., Berry, N. J., Boeckx, P., de Jong, B. H. J., DeVries, B., Girardin, C. A. J., Kearsley, E., Lindsell, J. A., Lopez-Gonzalez, G., Lucas, R., … Willcock, S. (2016). An integrated pan-tropical biomass map using multiple reference datasets. *Global Change Biology*, *22*, 1406–1420.

Béland, M., Baldocchi, D. D., Widlowski, J.-L., Fournier, R. A., & Verstraete, M. M. (2014). On seeing the wood from the leaves and the role of voxel size in determining leaf area distribution of forests with terrestrial LiDAR. *Agricultural and Forest Meteorology*, *184*, 82–97.

Boni Vicari, M., Disney, M., Wilkes, P., Burt, A., Calders, K., & Woodgate, W. (2019). Leaf and wood classification framework for terrestrial LiDAR point clouds. *Methods in Ecology and Evolution*, *10*, 680–694.

Bunce, R. G. H. (1968). Biomass and production of trees in a mixed deciduous woodland: I. Girth and height as parameters for the estimation of tree dry weight. *Journal of Ecology*, *56*, 759–775.

Burt, A., Boni Vicari, M., da Costa, A. C. L., Coughlin, I., Meir, P., Rowland, L., & Disney, M. (2021). New insights into large tropical tree mass and structure from direct harvest and terrestrial lidar. *Royal Society Open Science*, *8*, 201458.

Burt, A., Calders, K., Cuni-Sanchez, A., Gómez-Dans, J., Lewis, P., Lewis, S. L., Malhi, Y., Phillips, O. L., & Disney, M. (2020). Assessment of bias in Pan-tropical biomass predictions. *Frontiers in Forests and Global Change*, *3*, 12.

Burt, A., Disney, M., & Calders, K. (2018). Extracting individual trees from lidar point clouds using treeseg. *Methods in Ecology and Evolution*, *10*, 438–445.

Burt, A. P. (2017). *New 3D measurements of forest structure*. University College London.

Butt, N., Campbell, G., Malhi, Y., Fenn, M. M. K., & Thomas, M. (2009). *Initial results from establishment of a long-term broadleaf monitoring plot at Wytham Woods*. University of Oxford,Oxford, UK.

Butt, N., Slade, E., Thompson, J., Malhi, Y., & Riutta, T. (2013). Quantifying the sampling error in tree census measurements by volunteers and its effect on carbon stock estimates. *Ecological Applications*, *23*, 936–943. https://doi.org/10.1890/11-2059.1

Calders, K., Adams, J., Armston, J., Bartholomeus, H., Bauwens, S., Bentley, L. P., Chave, J., Danson, F. M., Demol, M., Disney, M., Gaulton, R., Krishna Moorthy, S. M., Levick, S. R., Saarinen, N., Schaaf, C., Stovall, A., Terryn, L., Wilkes, P., & Verbeeck, H. (2020). Terrestrial laser scanning in forest ecology: Expanding the horizon. *Remote Sensing of Environment*, *251*, 112102.

Calders, K., Burt, A., Newnham, G., Disney, M., Murphy, S., Raumonen, P., Herold, M., Culvenor, D., Armston, J., Avitabile, V., & Kaasalainen, M. (2015a). Reducing uncertainties in above-ground biomass estimates using terrestrial laser scanning. Paper presented at Silvi Laser 2015, La Grande Motte, France, 28–30 September 2015,.

Calders, K., Newnham, G., Burt, A., Murphy, S., Raumonen, P., Herold, M., Culvenor, D., Avitabile, V., Disney, M., Armston, J., & Kaasalainen, M. (2015). Nondestructive estimates of above-ground biomass using terrestrial laser scanning. *Methods in Ecology and Evolution*, *6*, 198–208.

Calders, K., Origo, N., Burt, A., Disney, M., Nightingale, J., Raumonen, P., Åkerblom, M., Malhi, Y., & Lewis, P. (2018). Realistic forest stand reconstruction from terrestrial LiDAR for radiative transfer modelling. *Remote Sensing*, *10*, 933.

Chave, J., Réjou-Méchain, M., Búrquez, A., Chidumayo, E., Colgan, M. S., Delitti, W. B. C., Duque, A., Eid, T., Fearnside, P. M., Goodman, R. C., Henry, M., Martínez-Yrízar, A., Mugasha, W. A., Muller-Landau, H. C., Mencuccini, M., Nelson, B. W., Ngomanda, A., Nogueira, E. M., Ortiz-Malavassi, E., … Vieilledent, G. (2014). Improved allometric models to estimate the aboveground biomass of tropical trees. *Global Change Biology*, *20*, 3177–3190.

Ciais, P., Schelhaas, M. J., Zaehle, S., Piao, S. L., Cescatti, A., Liski, J., Luyssaert, S., Le-Maire, G., Schulze, E.-D., Bouriaud, O., Freibauer, A., Valentini, R., & Nabuurs, G. J. (2008). Carbon accumulation in European forests. *Nature Geoscience*, *1*, 425–429.

Ciais, P., Tan, J., Wang, X., Roedenbeck, C., Chevallier, F., Piao, S.-L., Moriarty, R., Broquet, G., Le Quéré, C., Canadell, J. G., Peng, S., Poulter, B., Liu, Z., & Tans, P. (2019). Five decades of northern land carbon uptake revealed by the interhemispheric CO_2 gradient. *Nature*, *568*, 221–225.

Contestabile, M. (2012). Measurement challenges. *Nature Climate Change*, *2*, 563–565. https://doi.org/10.1038/nclimate1642

de Tanago Menaca, J. G., Lau, A., Bartholomeusm, H., Herold, M., Avitabile, V., Raumonen, P., Martius, C., Goodman, R., Disney, M., & Manuri, S., Others. (2018). Estimation of above-ground biomass of large tropical trees with Terrestrial LiDAR. *Methods in Ecology and Evolution*, *9*, 223–234.

Demol, M., Calders, K., Krishna Moorthy, S. M., Van den Bulcke, J., Verbeeck, H., & Gielen, B. (2021). Consequences of vertical basic wood density variation on the estimation of aboveground biomass with terrestrial laser scanning. *Trees*, *35*, 671–684.

Disney, M., Burt, A., Wilkes, P., Armston, J., & Duncanson, L. (2020). New 3D measurements of large redwood trees for biomass and structure. *Science Report*, *10*, 16721.

Duncanson, L., Armston, J., Disney, M., Avitabile, V., Barbier, N., Calders, K., Carter, S., Chave, J., Herold, M., MacBean, N., McRoberts, R., Minor, D., Paul, K., Réjou-Méchain, M., Roxburgh, S., Williams, M., Albinet, C., Baker, T., Bartholomeus, H., … Margolis, H. (2021). Aboveground Woody Biomass Product Validation Good Practices Protocol. Version 1.0. In L. Duncanson, M. Disney, J. Armston, J. Nickeson, D. Minor, & F. Camacho (Eds.), *Good Practices for Satellite Derived Land Product Validation*, (p. 236): Land Product Validation Subgroup (WGCV/CEOS), https://doi.org/10.5067/doc/ceoswgcv/lpv/agb.001

FAO. (2020). *Global forest resources assessment 2020*. Food and Agriculture Organization of the United Nations.

Fenn, K., Malhi, Y., Morecroft, M., Lloyd, C., & Thomas, M. (2015). The carbon cycle of a maritime ancient temperate broadleaved woodland at seasonal and annual scales. *Ecosystems*, *18*, 1–15.

Forestry Commission. (2014a). Carbon in live woodland trees in Britain.

Forestry Commission. (2014b). Biomass in live woodland trees in Britain.

Forestry Commission. (2013). NFI preliminary estimates of quantities of broadleaved species in British woodlands, with special focus on ash.

Friedlingstein, P., O'Sullivan, M., Jones, M. W., Andrew, R. M., Hauck, J., Olsen, A., Peters, G. P., Peters, W., Pongratz, J., Sitch, S., Le Quéré, C., Canadell, J. G., Ciais, P., Jackson, R. B., Alin, S., Aragão, L. E. O. C., Arneth, A., Arora, V., Bates, N. R., … Zaehle, S. (2020). Global carbon budget 2020. *Earth System Science Data*, *12*, 3269–3340.

Grassi, G., House, J., Dentener, F., Federici, S., den Elzen, M., & Penman, J. (2017). The key role of forests in meeting climate targets requires science for credible mitigation. *Nature Climate Change*, *7*, 220–226.

Hackenberg, J., Spiecker, H., Calders, K., Disney, M., & Raumonen, P. (2015). SimpleTree —An efficient open source tool to build tree models from TLS clouds, *Forests*, *6*, 4245–4294.

Hayashi, F. (2000). *Econometrics*. Princeton University Press.

Hubau, W., Lewis, S. L., Phillips, O. L., Affum-Baffoe, K., Beeckman, H., Cuní-Sanchez, A., Daniels, A. K., Ewango, C. E. N., Fauset, S., Mukinzi, J. M., Sheil, D., Sonké, B., Sullivan, M. J. P., Sunderland, T. C. H., Taedoumg, H., Thomas, S. C., White, L. J. T., Abernethy, K. A., Adu-Bredu, S., … Zemagho, L. (2020). Asynchronous carbon sink saturation in African and Amazonian tropical forests. *Nature*, *579*, 80–87.

JCGM. (2008). Evaluation of measurement data - guide to the expression of uncertainty in measurement (No. 100). https://www.iso.org/sites/JCGM/GUM/JCGM100/C045315e-html/C045315e.html?csnumber=50461

Jucker, T., Caspersen, J., Chave, J., Antin, C., Barbier, N., Bongers, F., Dalponte, M., van Ewijk, K. Y., Forrester, D. I., Haeni, M., Higgins, S. I.,

Holdaway, R. J., Iida, Y., Lorimer, C., Marshall, P. L., Momo, S., Moncrieff, G. R., Ploton, P., Poorter, L., … Coomes, D. A. (2017). Allometric equations for integrating remote sensing imagery into forest monitoring programmes. *Global Change Biology*, *23*, 177–190.

Kirby, K. J., (2020). The ash population in Wytham Woods. https://anhso.org.uk/wp-content/uploads/Fritillary/frit8-ashdieback.pdf

Kirby, K. J., Bazely, D. R., Goldberg, E. A., Hall, J. E., Isted, R., Perry, S. C., & Thomas, R. C. (2014). Changes in the tree and shrub layer of Wytham Woods (Southern England) 1974–2012: local and national trends compared. *Forestry*, *87*, 663–673.

Kirby, K. J., Smart, S. M., Black, H. I. J., Bunce, R. G. H., Corney, P. M., & Smithers, R. J. (2005). Long term ecological change in British woodland (1971–2001). *English Nature Research Reports*, *653*, 1–139.

Krishna Moorthy, S. M., Calders, K., Vicari, M. B., & Verbeeck, H. (2020). Improved supervised learning-based approach for leaf and wood classification From LiDAR point clouds of forests. *IEEE Transactions on Geoscience and Remote Sensing*, *58*, 3057–3070.

Laitinen, R. A. E., & Nikoloski, Z. (2019). Genetic basis of plasticity in plants. *Journal of Experimental Botany*, *70*, 739–745.

Lewis, S. L., Brando, P. M., Phillips, O. L., van der Heijden, G. M. F., & Nepstad, D. (2011). The 2010 Amazon drought. *Science*, *331*, 554.

Loubota Panzou, G. J., Fayolle, A., Jucker, T., Phillips, O. L., Bohlman, S., Banin, L. F., Lewis, S. L., Affum-Baffoe, K., Alves, L. F., Antin, C., Arets, E., Arroyo, L., Baker, T. R., Barbier, N., Beeckman, H., Berger, U., Bocko, Y. E., Bongers, F., Bowers, S., … Feldpausch, T. R. (2020). Pantropical variability in tree crown allometry. *Global Ecology and Biogeography*, *30*, 459–475. https://doi.org/10.1111/geb.13231

Matthews, G. (1993). Forestry commission technical paper 4: The carbon content of trees. *Forestry Commission*, .

McKay, H., Hudson, J. B., & Hudson, J., R. (2003). Woodfuel resource in Britain. FES B/W3/00787/REP/2 DTI/Pub URN 03/1436.

Mitchell, R. J., Beaton, J. K., Bellamy, P. E., Broome, A., Chetcuti, J., Eaton, S., Ellis, C. J., Gimona, A., Harmer, R., Hester, A. J., Hewison, R. L., Hodgetts, N. G., Iason, G. R., Kerr, G., Littlewood, N. A., Newey, S., Potts, J. M., Pozsgai, G., & Ray, D., … Woodward, S. (2014). Ash dieback in the UK: A review of the ecological and conservation implications and potential management options. *Biological Conservation*, *175*, 95–109.

Momo Takoudjou, S., Ploton, P., Sonké, B., Hackenberg, J., Griffon, S., de Coligny, F., Kamdem, N. G., Libalah, M., Mofack, G. I. I., Le Moguédec, G., Pélissier, R., & Barbier, N. (2018). Using terrestrial laser scanning data to estimate large tropical trees biomass and calibrate allometric models: A comparison with traditional destructive approach. *Methods in Ecology and Evolution*, *9*, 905–916.

Nabuurs, G. J., Masera, O., Andrasko, K., Benitez-Ponce, P., Boer, R., Dutschke, M., Elsiddig, E., Ford-Robertson, J., Frumhoff, P., Karjalainen, T., Krankina, O., Kurz, W. A., Matsumoto, M., Oyhantcabal, W., Ravindranath, N. H., Sanz Sanchez, M. J., & Zhang, X. (2007). Forestry. In B. Metz, O. R. Davidson, P. R. Bosch, R. Dave, & L. A. Meyer (Eds), *Climate change 2007: Mitigation. Contribution of Working Group III to the Fourth Assessment Report of the Intergovernmental Panel on Climate Change* (pp. 541–584). Cambridge University Press.

Needham, J., Merow, C., Butt, N., Malhi, Y., Marthews, T. R., Morecroft, M., & McMahon, S. M. (2016). Forest community response to invasive pathogens: the case of ash dieback in a British woodland. *Journal of Ecology*, *104*, 315–330.

Neyman, J., & Scott, E. L. (1960). Correction for bias introduced by a transformation of variables. *Annals of Mathematical Statistics*, *31*, 643–655.

Olvera Astivia, O. L., & Zumbo, B. D. (2019). Heteroskedasticity in multiple regression analysis: What it is, how to detect it and how to solve it with applications in R and SPSS. *Practical Assessment, Research, and Evaluation*, *24*, 1.

Pan, Y., Birdsey, R. A., Fang, J., Houghton, R., Kauppi, P. E., Kurz, W. A., Phillips, O. L., Shvidenko, A., Lewis, S. L., Canadell, J. G., Ciais, P., Jackson, R. B., Pacala, S. W., McGuire, A. D., Piao, S., Rautiainen, A., Sitch, S., & Hayes, D. (2011). A large and persistent carbon sink in the world's forests. *Science*, *333*, 988–993.

Picard, N., Rutishauser, E., Ploton, P., Ngomanda, A., & Henry, M. (2015). Should tree biomass allometry be restricted to power models? *For. Ecol. Manage.*, *353*, 156–163.

Ploton, P., Barbier, N., Momo, S. T., Réjou-Méchain, M., Bosela, F. B., Chuyong, G., Dauby, G., Droissart, V., Fayolle, A., Goodman, R. C., Henry, M., Kamdem, N. G., Mukirania, J. K., Kenfack, D., Libalah, M., Ngomanda, A., Rossi, V., Sonké, B., Texier, N., … Pélissier, R. (2016). Closing a gap in tropical forest biomass estimation: taking crown mass variation into account in pantropical allometries. *Biogeosciences*, *13*, 1571–1585.

Poorter, H., Jagodzinski, A. M., Ruiz-Peinado, R., Kuyah, S., Luo, Y., Oleksyn, J., Usoltsev, V. A., Buckley, T. N., Reich, P. B., & Sack, L. (2015). How does biomass distribution change with size and differ among species? An analysis for 1200 plant species from five continents. *New Phytology*, *208*, 736–749.

Poulsen, J. R., Medjibe, V. P., White, L. J. T., Miao, Z., Banak-Ngok, L., Beirne, C., Clark, C. J., Cuni-Sanchez, A., Disney, M., Doucet, J.-L., Lee, M. E., Lewis, S. L., Mitchard, E., Nuñez, C. L., Reitsma, J., Saatchi, S., & Scott, C. T. (2020). Old growth Afrotropical forests critical for maintaining forest carbon. *Global Ecology and Biogeography*, *29*, 1785–1798.

Python Software Foundation. (n.d.). Python Language Reference, version 3.7.6. https://www.python.org

Rackham, O. (2015). *Woodlands*. William Collins.

Raumonen, P., Kaasalainen, M., Åkerblom, M., Kaasalainen, S., Kaartinen, H., Vastaranta, M., Holopainen, M., Disney, M., & Lewis, P. (2013). Fast automatic precision tree models from terrestrial laser scanner data. *Remote Sensing*, *5*, 491–520.

Savill, P., Perrins, C., Kirby, K., & Fisher, N. (2011). *Wytham Woods: Oxford's ecological laboratory*. Oxford University Press.

Seidl, R., Thom, D., Kautz, M., Martin-Benito, D., Peltoniemi, M., Vacchiano, G., Wild, J., Ascoli, D., Petr, M., Honkaniemi, J., Lexer, M. J., Trotsiuk, V., Mairota, P., Svoboda, M., Fabrika, M., Nagel, T. A., & Reyer, C. P. O. (2017). Forest disturbances under climate change. *Nature Climate Change*, *7*, 395–402.

Smith, R. J. (1980). Rethinking allometry. *Journal of Theoretical Biology*, *87*, 97–111.

Vorster, A. G., Evangelista, P. H., Stovall, A. E. L., & Ex, S. (2020). Variability and uncertainty in forest biomass estimates from the tree to landscape scale: the role of allometric equations. *Carbon Balance Management*, *15*, 8.

Wang, D., Momo Takoudjou, & S., Casella, E. (2020). LeWoS: A universal leaf-wood classification method to facilitate the 3D modelling of large tropical trees using terrestrial LiDAR. *Methods in Ecology and Evolution*, *11*, 376–389.

Wilkes, P., Lau, A., Disney, M., Calders, K., Burt, A., Gonzalez de Tanago, J., Bartholomeus, H., Brede, B., & Herold, M. (2017). Data acquisition considerations for terrestrial laser scanning of forest plots. *Remote Sensing of Environment*, *196*, 140–153.

Zanne, A. E., Lopez-Gonzalez, G., Coomes, D. A., Ilic, J., Jansen, S., Lewis, S. L., Miller, R. B., Swenson, N. G., Wiemann, M. C., & Chave, J. (2009). Data from: Towards a worldwide wood economics spectrum. https://doi.org/10.5061/dryad.234

Zhou, X., Yang, M., Liu, Z., Li, P., Xie, B., & Peng, C. (2021). Dynamic allometric scaling of tree biomass and size. *Nature Plants*, *7*, 42–49.

Zianis, D., Muukkonen, P., Mäkipää, R., & Mencuccini, M. (2005). Biomass and stem volume equations for tree species in *Europe. Silva Fennica Monographs*, *4*, The Finnish Society of Forest Science and The Finnish Forest Research Institute.

SUPPORTING INFORMATION

Additional supporting information can be found online in the Supporting Information section at the end of this article.

Supplementary table S1: Overview of studies and reports that apply the Bunce allometric AGB models.

Supplementary table S2: Species-specific wood density values used for conversion of QSM volume to woody biomass

Supplementary figure S1: Location of the 1.4 ha study area in Wytham Woods (grey box).

Supplementary figure S2: Examples of extracted individual trees and their reconstructed QSMs using *TreeQSM*.

Supplementary figure S3: AGB residuals for individual tree AGB for Wytham Woods: allometric AGB using Bunce allometric models minus TLS-derived AGB

Supplementary table S3: Structural characteristics of *A. pseudoplatanus* and all trees within the Wytham Woods study area

Supplementary table S4: Model parameters and bootstrapped 95% confidence intervals for the 3 model forms for *A. pseudoplatanus* and all trees within the Wytham Woods study area. $\hat{\sigma}$is the estimated standard deviation

Supplementary table S5: Uncertainty and bias from these models following a repeated (10 times) stratified 10-fold cross-validation are calculated using median symmetric accuracy (MSA) and the symmetric signed percentage bias (SSPB)

Supplementary figure S4: Regression diagnostics for the 3 model fits for *Acer pseudoplatanus*

Supplementary figure S5: Regression diagnostics for the 3 model fits for all trees

Supplementary figure S6: Tree diameter (*D*), tree height (*H*) and vertical projected crown area (*CA*) for 815 living trees in Wytham Woods derived from TLS data

Supplementary figure S7: The 10 percent smallest trees in terms of volume were iteratively removed and the multivariate model *m2* was refitted

Supplementary figure S8: The 10 percent smallest trees in terms of volume were iteratively removed and the multivariate model *m3* was refitted

How to cite this article: Calders, K., Verbeeck, H., Burt, A., Origo, N., Nightingale, J., Malhi, Y., Wilkes, P., Raumonen, P., Bunce, R. G. H., & Disney, M. (2022). Laser scanning reveals potential underestimation of biomass carbon in temperate forest. *Ecological Solutions and Evidence*, *3*, e12197. https://doi.org/10.1002/2688-8319.12197